Proceedings of the 16th International Conference on Soil Mechanics and Geotechnical Engineering

doi:10.3233/978-1-61499-656-9-1071

Viscous deformation of geogrid-reinforced sand in plane strain compression

Propriétés visqueuses d'un sable renforcé par géogrille à partir d'essais de compression à déformations planes

W. Kongkitkul & F. Tatsuoka
Department of Civil Engineering, Tokyo University of Science, Japan

ABSTRACT

The viscous properties of a polymer geogrid reinforcement and Toyoura sand were separately evaluated by changing stepwise the strain rate as well as performing sustained loading and load/stress relaxation tests during otherwise monotonic loading in, respectively, tensile loading tests and plane strain compression (PSC) tests. The viscous properties of the two materials were formulated and simulated in the framework of a non-linear three-component rheology model. The viscous properties of geogrid-reinforced Toyoura sand in PSC were evaluated. Strains in the geogrid were evaluated by the photogrametric method. The time history of tensile force in the geogrid during sustained loading at a constant external load obtained by analysing the measured time history of strains showed that the tensile force in the geogrid decreased with time. In that case, the possibility of ultimate creep rupture of the geogrid is very low.

RÉSUMÉ

Les propriétés visqueuses d'un renforcement par géogrille à base de polymères et du sable de Toyoura ont été estimées de manière séparée. Ces propriétés ont été déterminées à partir d'essais monotones de traction et de compression à déformations planes en effectuant des changements de vitesse de déformation, des relaxations en contrainte et déformation ou par maintien du chargement. D'une part, les propriétés visqueuses des deux matériaux ont été exprimées et simulées dans le cadre d'un modèle rhéologique à trois composantes. D'autre part, celles du sable de Toyoura renforcé par géogrille ont été évaluées lors d'essais de compression à déformations planes, les déformations de la géogrille étant estimées par méthode photographique. L'évolution avec le temps de la force de traction dans la géogrille, lors du maintien du chargement à charge externe constante, a été obtenue à partir de l'analyse de celle des déformations mesurées. Il est montré que la force de traction dans la géogrille décroit avec le temps, ce qui laisse une faible possibilité de rupture ultime de la géogrille par fluage.

1 INTRODUCTION

A great number of permanent geosynthetic-reinforced soil (GRS) structures were constructed because of their high cost-effectiveness and seismic stability (e.g. Tatsuoka et al., 1997). To predict residual deformation of a GRS structure during service, it is first necessary to evaluate the viscous property of geosynthetic and backfill. Di Benedetto et al. (2002) and Tatsuoka et al. (2002) studied the viscous property of sand, while Hirakawa et al. (2003) and Kongkitkul et al. (2004) studied that of geosynthetic. However, the viscous property of geogrid-reinforced sand, which is very complicated due to an interaction between the viscous properties of these two components, have not been investigated. In the present study, this issue was studied by extending previous studies on the effects of the stiffness, surface roughness and covering ratio (CR) of geogrid on the deformation and strength characteristics of reinforced sand in plane strain compression (PSC) (Tatsuoka & Yamauchi, 1986; Kotake et al., 1999; Peng et al., 2000).

2 TEST MATERIALS AND APPARATUSES

The tensile load-tensile strain property of the Polyester geogrid used in the PSC tests was evaluated by special tensile loading tests (Fig. 1a). The specimen consisted of five strands with a centre-to-centre distance equal to 9 mm. In these tensile loading tests (and PSC tests on unreinforced and reinforced sand described below), monotonic loading (ML) tests were performed on different specimens, while the strain rate was changed stepwise and sustained loading and stress relaxation tests were performed during otherwise ML at a constant strain rate. Figure 2 shows a typical result (the simulation will be explained later).

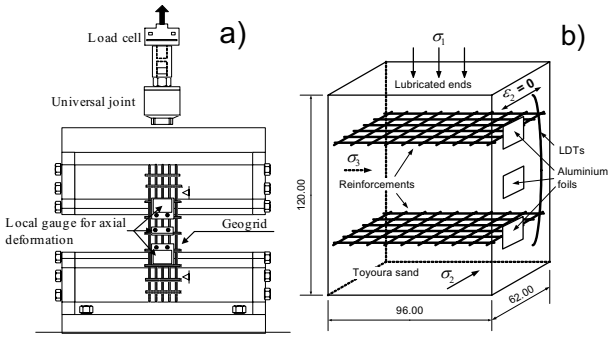

Figure 1. a) Geogrid specimen in tensile loading test; and b) reinforced sand specimen in PSC test.

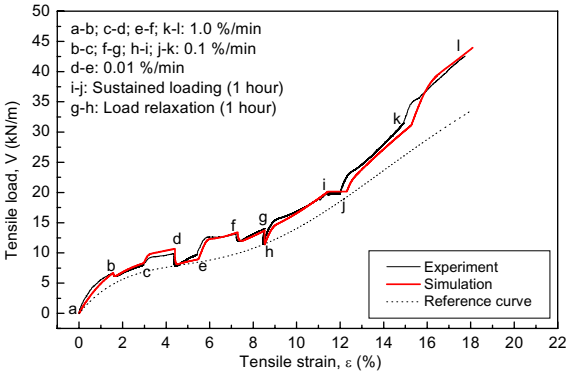

Figure 2. Tensile load-tensile strain relation of PET geogrid.

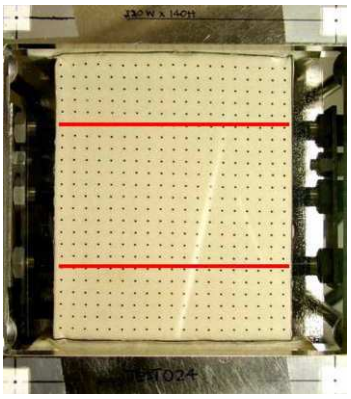

Figure 3. σ_2-surface of reinforced sand specimen.

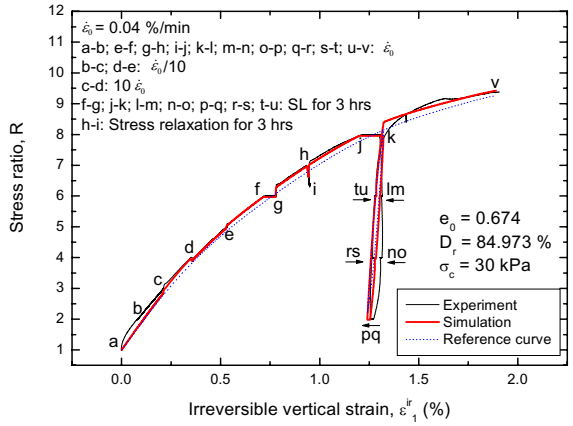

Figure 4. $R = \sigma_1/\sigma_3$-ε^{ir}_1 relation of Toyoura sand obtained from PSC test.

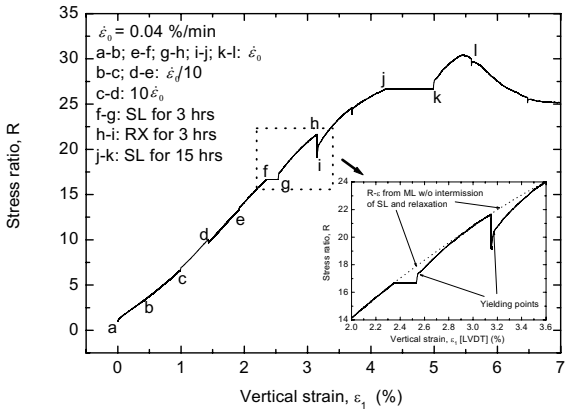

Figure 5. Average R-average ε_1 relation obtained from a PSC test of reinforced Toyoura sand.

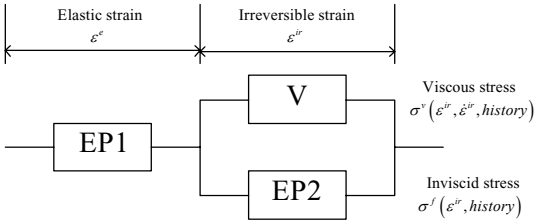

Figure 6. Non-linear three-component rheology model.

PSC tests were performed on air-dried Toyoura sand (D_{50} = 0.2 mm). Air-pluviated specimens (D_r = 84 – 88 %) were 96 mm [W] x 62 mm [D] x 120 mm [H] (Fig. 1b). Inside geogrid-reinforced sand specimens, having the same dimensions with the unreinforced ones, two geogrid layers were arranged, each having six and ten strands in the longitudinal and transverse directions. The σ_1 and σ_2 ends of the PSC specimens were well lubricated. In all the tests, the measured friction on the σ_2 surfaces was very small. Confining pressure of 30 kPa was applied by partial vacuuming. The vertical strain was measured by using a LVDT and a pair of LDTs while the horizontal strain was measured by using three pairs of proximity transducers. A number of pictures of a 0.3 mm-thick specimen membrane of latex rubber on the σ_2 surface with a number of printed markers were taken through the Acrylic confining platen during each test (Fig. 3). Figures 4 & 5 show typical results for unreinforced and reinforced sand specimens. A global unloading and reloading cycle with several sustained loading stages was applied to the unreinforced sand. The stress and strain values shown in Fig. 5 are those averaged for the whole of specimen.

3 NON-LINEAR THREE-COMPONENT MODEL

The test results were analysed in the framework of a non-linear three-component model (Fig. 6; Di Benedetto et al., 2002; Tatsuoka et al., 2002). The stress, σ, consists of inviscid and viscous components, σ^f and σ^v, while the strain increment, $d\varepsilon$, consists of elastic and irreversible components, $d\varepsilon^e$ and $d\varepsilon^{ir}$. The following four different types of σ^v have been found relevant for different types of geomaterial (i.e. soil and rock) and geosynthetic:

Isotach viscosity: The current value of σ^v is a unique function of ε^{ir} and its rate, $\dot{\varepsilon}^{ir}$, as long as ML continues, while the change of σ^v upon a change in $\dot{\varepsilon}^{ir}$ is persistent with an increase in ε^{ir}. Therefore, the stress-strain curves for ML at different constant strain rates are separated from each other and the separation increases with an increase in σ^f. This type is relevant to many types of geosynthetic (Hirakawa et al., 2003; Kongkitkul et al., 2004).

TESRA viscosity: The current value of σ^v is a function of not only ε^{ir} and $\dot{\varepsilon}^{ir}$, but also loading history even in the case of ML, while the change of σ^v upon a change in $\dot{\varepsilon}^{ir}$ decays with an increase in ε^{ir}. Therefore, stress-strain relations for ML at different constant strain rates tend to collapse into a single relation (called the reference relation). This type is relevant to Toyoura sand.

General TESRA viscosity: Like the TESRA type, the change of σ^v upon a change in $\dot{\varepsilon}^{ir}$ decays with ε^{ir}, but the decay rate increases with an increase in ε^{ir} changing the viscosity type from Isotach type at small strains towards the TESRA type at large strains.

Combined viscosity: σ^v consists of the Isotach and general TESRA σ^v components. This is the most flexible type, including the three types above, and relevant to the Polyester geogrid used in the present study.

4 RESULTS AND ANALYSIS BY THE MODEL

The following trends, common to the geogrid and Toyoura sand, may be seen from Figs. 2 & 4:

1) The tensile load and the stress ratio suddenly change upon a stepwise change in the strain rate, $\dot{\varepsilon}$, showing noticeable effects of material viscosity.
2) The change in the load/stress upon a step change in $\dot{\varepsilon}$ decays with an increase in the strain, ε. The decay rate increases with ε for the geogrid (the combined type), while it is constant and consistently large with Toyoura sand (the TESRA type).
3) After ML is restarted at the original constant strain rate following sustained loading and stress relaxation, the stiffness of load/stress-strain relation is very high, close to the elastic value, for some range of load/stress.

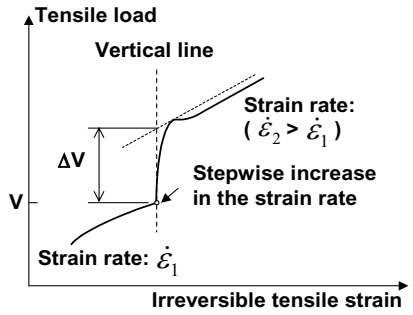

Figure 7. Definition of load jump.

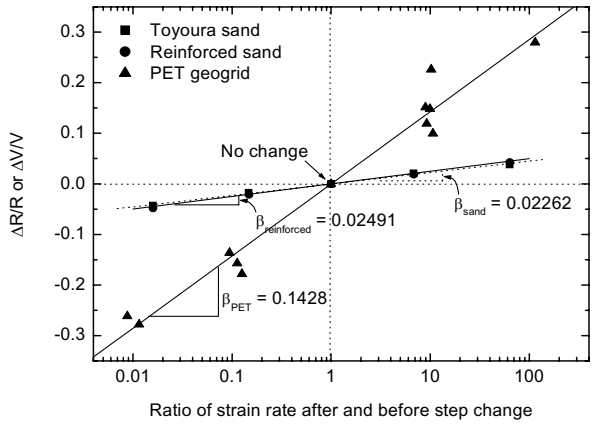

Figure 8. β-value plots for different materials.

4) Creep deformation taking place during sustained loading and load/stress relaxation at a constant strain are noticeable.

The material viscosity can be quantified in terms of the slope β of the relation between "the ratio of the load/stress jump to the current load/stress" (Fig. 7) and "the logarithm of the ratio of the irreversible strain rates after/before a stepwise change" (Fig. 8). The β value of the Polyester geogrid is much higher than that of Toyoura sand in PSC. It may be seen by comparing Figs. 2 & 4, however, that the general trend of viscosity is very similar with these two very different materials.

As seen by comparing Figs. 4 & 5, the strength of sand increased by reinforcing about three times, while the axial strain at peak increased about 2.5 times. The reinforced sand also exhibited noticeable viscous behaviour, which is very similar to those of sand and geogrid. Moreover, the β value from the R-ε_l relation of the reinforced sand is very similar to that of unreinforced sand (Fig. 8). This is because the viscous property of the geogrid is reflected in the ε_l values only indirectly. However, the following trend of viscous behaviour is obviously different between the two materials (geogrid and sand) and the reinforced sand. That is, with geogrid and sand, when ML is restarted after sustained loading and load/stress relaxation, the V-ε and R-ε_l relations first slightly overshoot and then return to the primary relations that would be obtained from continuous ML. On the other hand, the R-ε_l relation of the reinforced sand exhibits yielding at a stress level much lower than the primary loading relation. This should be explained by the fact that the tensile load of geogrid arranged in sand is controlled by the following three factors: a) an increase imposed by an increase in the viscous lateral tensile strain of sand caused by constant sustained vertical loading; b) a decrease associated with the development of viscous lateral compressive strain of sand caused by the tensile force of the geogrid; and c) a decrease due to the load relaxation of geogrid that would take place even under constant tensile strain. The data presented in Fig. 5 suggests that, during the sustained loading, the tensile load in the geogrid arranged in

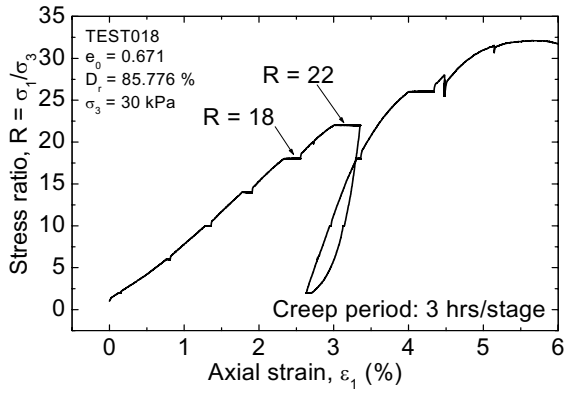

Figure 9. R-ε_l relation from PSC test on reinforced sand with multiple sustained loading stages.

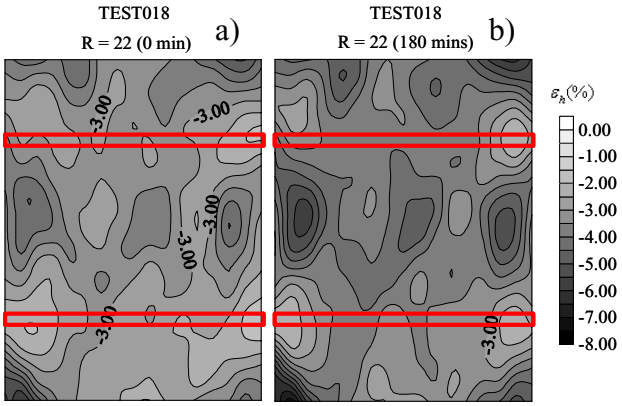

Figure 10a & b. Horizontal strain contours.

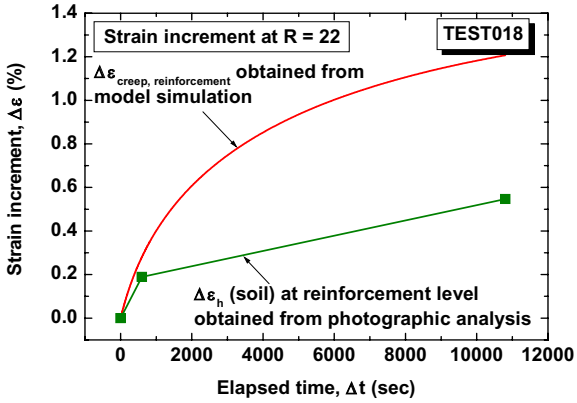

Figure 11. Time histories of strain of geogrid during sustained loading of reinforced sand.

the sand decreased with time because factors b & c overwhelmed factor a.

To confirm this inference, another ML PSC test at the same strain rate as shown in Fig. 5, with several sustained loading stages, was performed on reinforced sand (Fig. 9). Figures 10a & b show the lateral strain fields at the start and the end (at an elapsed time of 180 minutes) of sustained loading at R = 22, obtained by the photogrametric analysis. The local lateral strains around the geogrid layers were relatively small due to the restraining effects of the geogrid. The tensile strains of the geogrid were evaluated by assuming that the horizontal strains of the sand zone located at the geogrid layers are the same as those of the geogrid. The time history of the tensile strain averaged for the whole length of each geogrid layer was obtained as presented in Fig. 11.

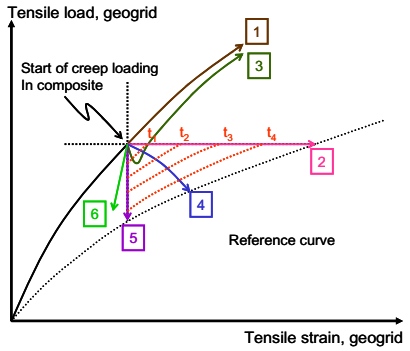

Figure 12. Tensile load-strain relations of geogrid arranged in sand subjected to sustained loading.

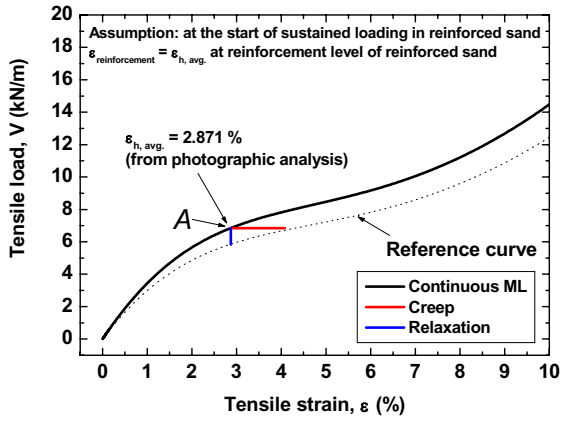

Figure 13. Generated tensile load-strain relation of geogrid with specified loading histories.

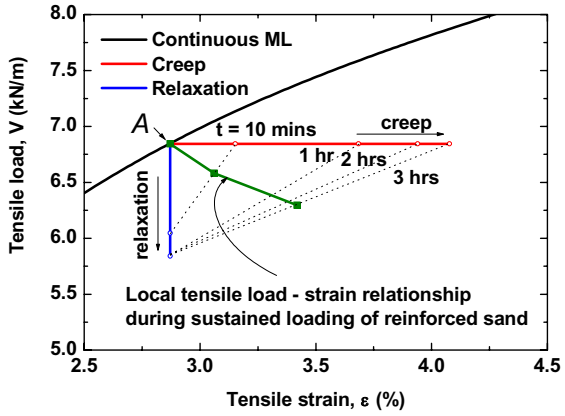

Figure 14. Tensile load-strain relations of geogrid arranged in sand subjected to sustained loading.

Figure 12 illustrates different possible load-strain curves (*2* - *6*) of a geogrid arranged in sand when subjected to sustained loading during otherwise ML at a constant strain rate (*1*). That is, *2*) tensile load is constant (i.e. sustained loading); *3*) the strain rate is constant and lower than the one during the ML; and *4*) the tensile load decreases with time. Moreover, other typical load-strain histories are: *5*) the tensile load relaxes at a constant strain; and *6*) unloading with a negative tensile strain rate takes place. The case *4*) is relevant to the sustained loading stage at R = 22, presented in Fig. 9, as shown below.

As shown in Figs. 2 & 4, the three-component model (Fig. 6) can simulate very well the viscous behaviour of geogrid and sand. The viscosity parameters were determined based on the β values (Fig. 8) and the reference relation (V^f-ε and R^f-ε_1 relations) were determined to fit the overall behaviour. By simulation using these model parameters, the load-strain relation of geogrid in ML at a strain rate of 0.047 %/minute was obtained (Fig. 13). This strain rate was evaluated from a tensile strain increment between R = 18 and 22 obtained by the photogrametric method. The time histories of tensile strain during the sustained loading test and tensile load during the load relaxation test, both starting from point ***A*** in Fig. 13, were obtained by the numerical simulation. The simulated and measured time histories of strain of geogrid during the sustained loading at a constant tensile load are compared in Fig. 11. The measured tensile strain was much smaller than the one during the sustained load. Then, the load-strain relation of geogrid during the sustained loading test of reinforced sand (Fig. 10) and those during sustained loading and load relaxation of the geogrid (Fig. 13) were obtained (Fig. 14). Linear contours at elapsed times equal to 10 minutes; 1 hour; 2 hours; and 3 hours were obtained for the first approximation. The load-strain relation of geogrid during the sustained loading of reinforced sand was obtained by substituting the known strain values at these selected elapsed times into the contours. These results indicate that the tensile load of geogrid decreased with time during the sustained loading test of reinforced sand.

5 CONCLUSIONS

The following conclusions could be derived:

1) Both geogrid and sand have noticeable viscous properties. The test results were simulated very well by a non-linear three-component rheology model.
2) Geogrid-reinforced sand exhibited a significant trend of viscous behaviour. The test results and their analysis by the three-component model indicated that the tensile force in the geogrid decreased with time during sustained loading of reinforced sand.

The second conclusion suggests that it could be highly conservative to assume that the tensile force of a geogrid arranged in the backfill is maintained constant during service at constant working load.

REFERENCES

Di Benedetto, H., Tatsuoka, F. and Ishihara, M. 2002. Time-dependant shear deformation characteristics of sand and their constitutive modelling. *Soils and Foundations*, 42(2), 1-22.

Hirakawa, D., Kongkitkul, W., Tatsuoka, F. and Uchimura, T. 2003. Time-dependent stress-strain behaviour due to viscous properties of geosynthetic reinforcement. *Geosynthetics International*, 10(6), 176-199.

Kongkitkul, W., Hirakawa, D., Tatsuoka, F. and Uchimura, T. 2004. Viscous deformation of geosynthetic reinforcement under cyclic loading conditions and its model simulation. *Geosynthetics International*, 11(2), 73-99.

Kotake, N., Tatsuoka, F., Tanaka, T., Siddiquee, M.S.A. and Yamauchi, H. 1999. An insight into the failure of reinforced sand in plane strain compression by FEM simulation. *Soils and Foundations*, 39(5), 103-130.

Peng, F.L., Kotake, N., Tatsuoka, F., Hirakawa, D. and Tanaka, T. 2000. Plane strain compression behaviour of geogrid-reinforced sand and its numerical analysis. *Soils and Foundations*, 40(3), 55-74.

Tatsuoka, F. and Yamauchi, H. 1986. A reinforcing method for steep clay slopes with a non-woven fabric. *Geotextiles and Geomembranes*, 4(3/4), 241-268.

Tatsuoka, F., Tateyama, M., Uchimura, T. and Koseki, J. 1997. Geosynthetic-reinforced soil retaining walls as important permanent structures, 1996-1997 Mercer Lecture. *Geosynthetics International*, 4(2), 81-136.

Tatsuoka, F., Ishihara, M., Di Benedetto, H. and Kuwano, R. 2002. Time-dependent shear deformation characteristics of geomaterials and their simulation. *Soils and Foundations*, 42(2), 106-132.